THERMOGRAPHIC IMAGING OF DEFECTS IN ANISOTROPIC COMPOSITES

Y.A. Plotnikov and W.P. Winfree
M.S. 231
NASA Langley Research Center
Hampton, VA 23681-0001

INTRODUCTION

Composite materials are of increasing interest to the aerospace industry as a result of their weight versus performance characteristics. One of the disadvantages of composites is the high cost of fabrication and post inspection with conventional ultrasonic scanning systems. The high cost of inspection is driven by the need for scanning systems which can follow large curve surfaces. Additionally, either large water tanks or water squirters are required to couple the ultrasonics into the part. Thermographic techniques offer significant advantages over conventional ultrasonics by not requiring physical coupling between the part and sensor. The thermographic system can easily inspect large curved surface without requiring a surface following scanner. However, implementation of Thermal Nondestructive Evaluations (TNDE) for flaw detection in composite materials and structures requires determining its limit.

Advanced algorithms have been developed to enable locating and sizing defects in carbon fiber reinforced plastic (CFRP). Thermal Tomography is a very promising method for visualizing the size and location of defects in materials such as CFRP [1, 2]. However, further investigations are required to determine its capabilities for inspection of thick composites.

In present work we have studied influence of the anisotropy on the reconstructed image of a defect generated by an inversion technique. The composite material is considered as homogeneous with macro properties: thermal conductivity K, specific heat c, and density ρ. The simulation process involves two sequential steps: solving the three dimensional transient heat diffusion equation for a sample with a defect, then estimating the defect location and size from the surface spatial and temporal thermal distributions (inverse problem), calculated from the simulations.

MODEL FOR THERMAL TOMOGRAPHY IN ANISOTROPIC MATERIAL

To simulate the thermographic inspection, the diffusion of heat after flash heating of the whole top surface has been modeled. The composite is represented as a flat plate of thickness D_z with thermal properties of the composite material. A subsurface defect is

represented as a non-conductive void with a rectangular cross section $l_x \times l_y$. The void extends from bottom of the plate, has a thickness h, and located a distance d below the surface (Fig. 1a). The rectangular shape of the defect has been chosen to assess the extent of the "rounding" effect of the thermal propagation process.

For purpose of simplicity, the plate is assumed to have only three non-zero principal conductivities $K_{11} = K_x$, $K_{22} = K_y$, and $K_{33} = K_z$ of 3x3 matrix of thermal conductivity K and axis of the Cartesian coordinate system $0xyz$ are the principal axis of conductivity [3]. With these assumptions, the unsteady heat diffusion equation has the form:

$$\frac{\partial T}{\partial t} = \alpha_x \frac{\partial^2 T}{\partial x^2} + \alpha_y \frac{\partial^2 T}{\partial y^2} + \alpha_z \frac{\partial^2 T}{\partial z^2}, \tag{1}$$

where $\alpha_i = K_i / \rho c$ is coefficient of thermal diffusivity and index i is x, y, and z directions respectively. A modified alternating direction implicit scheme, introduced by Douglas and Gunn, has been used to solve equation (1). The scheme is unconditionally stable and has second-order accuracy in space and time for three-dimensional heat diffusion equation [4]. The temperature distribution from a time level t to the next level $t + \Delta t$ is calculated by a three step algorithm described in detail elsewhere [4].

The size of the finite difference grid is 100 x 50 x 25 knots with geometrical size of 100 mm x 50 mm x 25 mm. It gives the spatial resolution of 1 mm in each directions. By maintaining sample symmetry, only one half of the sample needs to be represented by the simulation (Fig. 1a).

In second stage, the shape of the defect is reconstructed using a time dependent sequence of thermal contrast distributions. To solve the inverse problem, a variant of the thermal tomography technique, described by Maldague [2] in section 6.3.4 is applied. The thermal contrast is given by

$$C = \frac{T_{def}(t) - T_{def}(0)}{T_{soa}(t) - T_{soa}(0)} - 1, \tag{2}$$

a)   b)
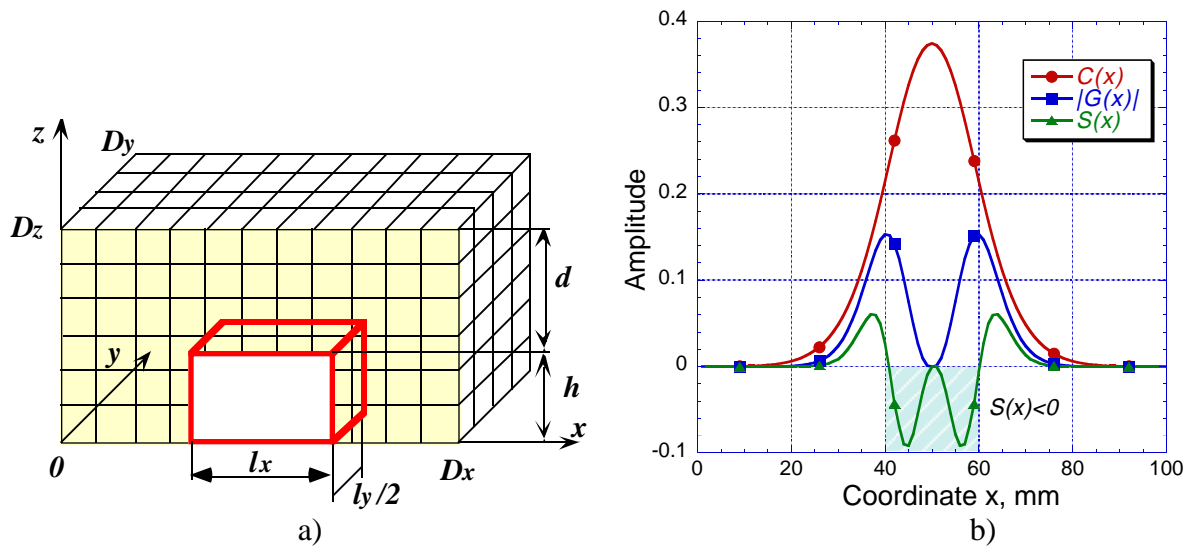
Figure 1. Model of the defect a) and algorithm for planar size extraction b).

where $T_{def}(t)$ is the thermal response of the surface above the defect and $T_{soa}(t)$ is the thermal response of the sound area. The subtraction of 1 in the equation (2) is convenient since $C \to 0$ when defect is absent and increases with greater difference between defect and sound regions. For simulations the initial temperature distribution before heating is $T_{def}(0) = T_{soa}(0) = 0$.

The evaluated object has been separated to 12 2-mm layers in depth corresponding to the diffusion time of the thermal flux. For each time gate thermograms were averaged into slices, which represent the layers from the top surface to the bottom of the plate. The shape of the defect in each layer is determined from the gradient of the averaged temperature contrast [2]. A point in the layer belongs to the defect if the partial derivatives of the contrast $C(x, y)$ and the magnitude of the gradient of the contrast $|\nabla C|$ in x direction for this point have opposite signs. Defining a function $S(x, y)$ as

$$S(x, y) = \frac{\partial C}{\partial x} \cdot \frac{\partial |\nabla C|}{\partial x}, \tag{3}$$

then a defect underlies a given point in the image if $S(x, y) \le 0$ (Fig. 1b). The reconstruction of defect shape is automatic and does not require prior information about the defect location. The accuracy of the temperature calculations yields defect contours almost in all layers. A thresholding procedure establishes which layers have no defects. For layer n if $C < M/n^2$ then no defect shape is reconstructed for that layer, where M is the empirically determined coefficient depending on the thermal properties of the material.

The reconstructed image of the plate contains binary information about all 12 layers and can be plotted in three-dimensional form by mathematical software packages (e.g. Mathematica™). This method enables visualization of a defect and a direct comparison of the reconstructed size of the defect and the defect parameters input into the simulations.

RESULTS OF SIMULATIONS

It is important to investigate the capability of the proposed inverse algorithm for automated defect detection. The only manual input required in the algorithm is the specification of a point located in a sound region, which is necessary to calculate the contrast in equation (2). The described algorithm allows a determination of the depth of a defect in the isotropic plate to within 2 mm. Preliminary results obtained with the program have shown that the reconstructed shapes of two separate defects are close to their actual shapes when the defects are separated by a distance greater than two times their depth. Fig. 2 represents the 12 layers (upper 24 mm) of the 100 mm x 100 mm x 25 mm plate with the reconstructed images of two defects. One defect with a planar size of 10 mm x 60 mm is located 5 mm below the surface and the second defect is 20 mm x 20 mm and 15 mm below surface. Reconstructions were curried out for a separation distance of 10 mm (Fig. 2a) and no separation (Fig. 2b). This latter case can be considered to present a single defect with a complex shape. As seen in the figure, the algorithm works well for both cases, although the orthorhombic shape is reconstructed far better for the shallowest defect. The reconstruction process also generates visible noise located between the defect and the nearest adiabatic boundary. This is thought to be a combined result of thresholding and size extraction procedures.
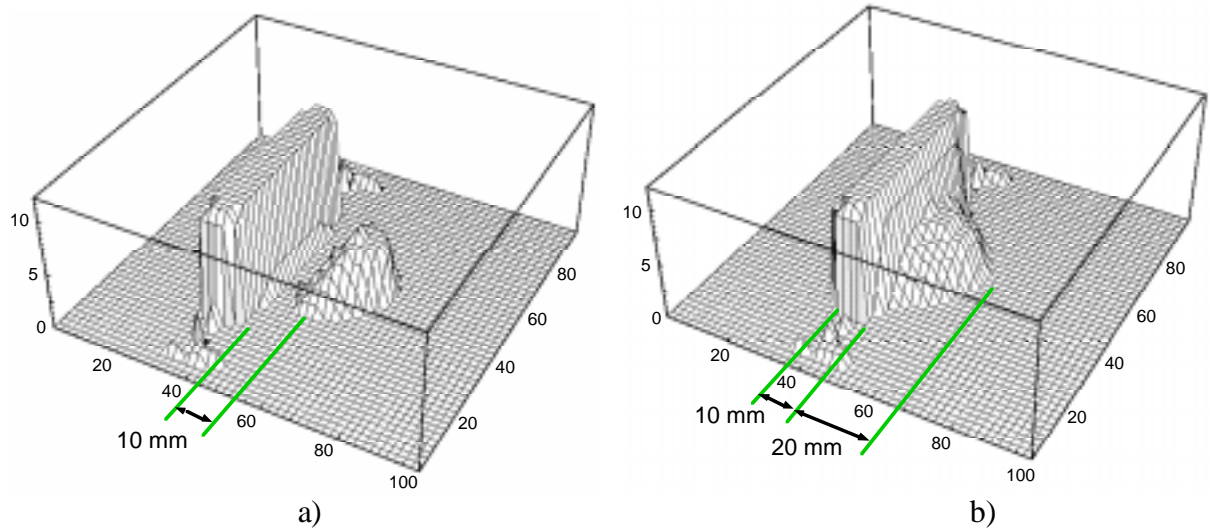
a)   b)

Figure 2. Reconstructed image of two defects: 10 mm x 60 mm, 5 mm below surface and 20 mm x 20 mm, 15 mm below the surface located on a distance 10 mm a) and connected to each other b).

The effect of anisotropy has been investigated by varying value of thermal diffusivity in orthogonal directions. The measurements of thermal diffusivity on samples, cut from stitched composite structure, have been made in three perpendicular directions using a flash-heating method. The typical values measured for the composite are: $\alpha_x = 1.7 \cdot 10^{-6} m^2/s$ (perpendicular to the stitches), $\alpha_y = 2.8 \cdot 10^{-6} m^2/s$ (parallel to the stitches), $\alpha_z = 0.7 \cdot 10^{-6} m^2/s$ (perpendicular to the ply direction). Initially, the differences in the thermal diffusivity in the plane of the ply are neglected (α_x and α_y are set to $2.8 \cdot 10^{-6} m^2/s$) to simplify the calculations. α_z has been varied in order to assess the influence of anisotropy. Calculations were performed for different values of the effusivity ratio, defined as

$$\frac{e_x}{e_z} = \frac{\sqrt{K_x \rho c}}{\sqrt{K_z \rho c}} = \sqrt{\frac{\alpha_x}{\alpha_z}}, \qquad (4)$$

where e_x and e_z are the effusivities in the x and z directions respectively. Three cases were simulated:

1) a material with thermal properties inverted relative to CFRP: $\alpha_z = 11.2 \cdot 10^{-6} m^2/s$, $e_x/e_z = 0.5$;

2) an isotropic material: $\alpha_z = 2.8 \cdot 10^{-6} m^2/s$, $e_x/e_z = 1$;

3) CFRP: $\alpha_z = 0.7 \cdot 10^{-6} m^2/s$, $e_x/e_z = 2$.

The reconstructed images of a defect 20 mm x 20 mm x 10 mm located 15 mm below the surface for these values of the effusivities ratio are presented in Fig. 3a-c. As can be seen from this figure, the planar size of the reconstructed defect increases with rising effusivity ratio. The "rounding" effect is especially strong for $e_x/e_z = 2$.

Fig. 3d presents the reconstructed image of the same defect in the plate for the most complicated case when all three x, y, and z components of the diffusivity are different, having
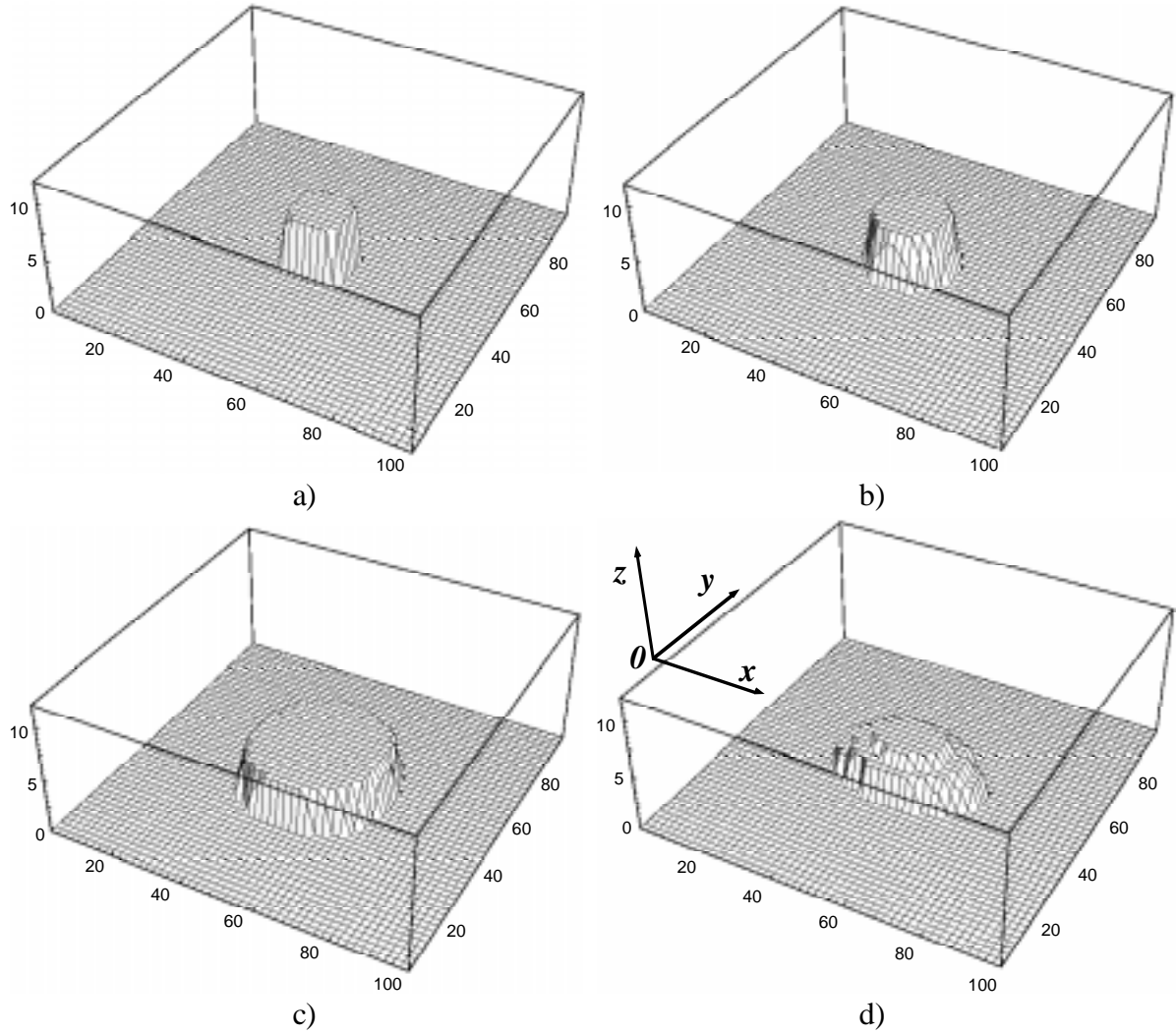
Figure 3. Reconstructed image of the plate with the defect 20 mm x 20 mm and 15 mm below the surface for different values of e_x/e_z: a) $e_x/e_z = 0.5$; b) $e_x/e_z = 1$; c) $e_x/e_z = 2$; d) $e_x/e_z = 2$, $e_x/e_y = 1.41$.

values equal to the measured values listed previously. The planar anisotropy yields a defect shape with an increased size in the direction of the higher value of diffusivity. The distortion of the planar shape of a defect image in anisotropic composites has been reported by other authors working with CFRP specimens [2,5]. This provides addition problems for the task of size estimation for a real defect with unknown thermophysical and geometrical properties.

Fig. 4a-c depict graphs of the ratio l_a/l of a square defect, where l_a is the reconstructed size and l is the actual size of the defect. As expected, the higher value of thermal conductivity along the surface results in a larger apparent size for the defect. As can be seen in Fig. 4a-c, the smaller the defect, the greater the influence of the anisotropy on the apparent size of the defect. The increase of the apparent size with increasing depth for $e_x/e_z = 1$ (isotropic material) is a result of application of the peak gradient criteria of thermal contrast for size extraction. Analyzing these graphs, we have concluded that the size, extracted on this basis, is only accurate for defect size where the width $l > 2d \cdot e_z/e_x$.
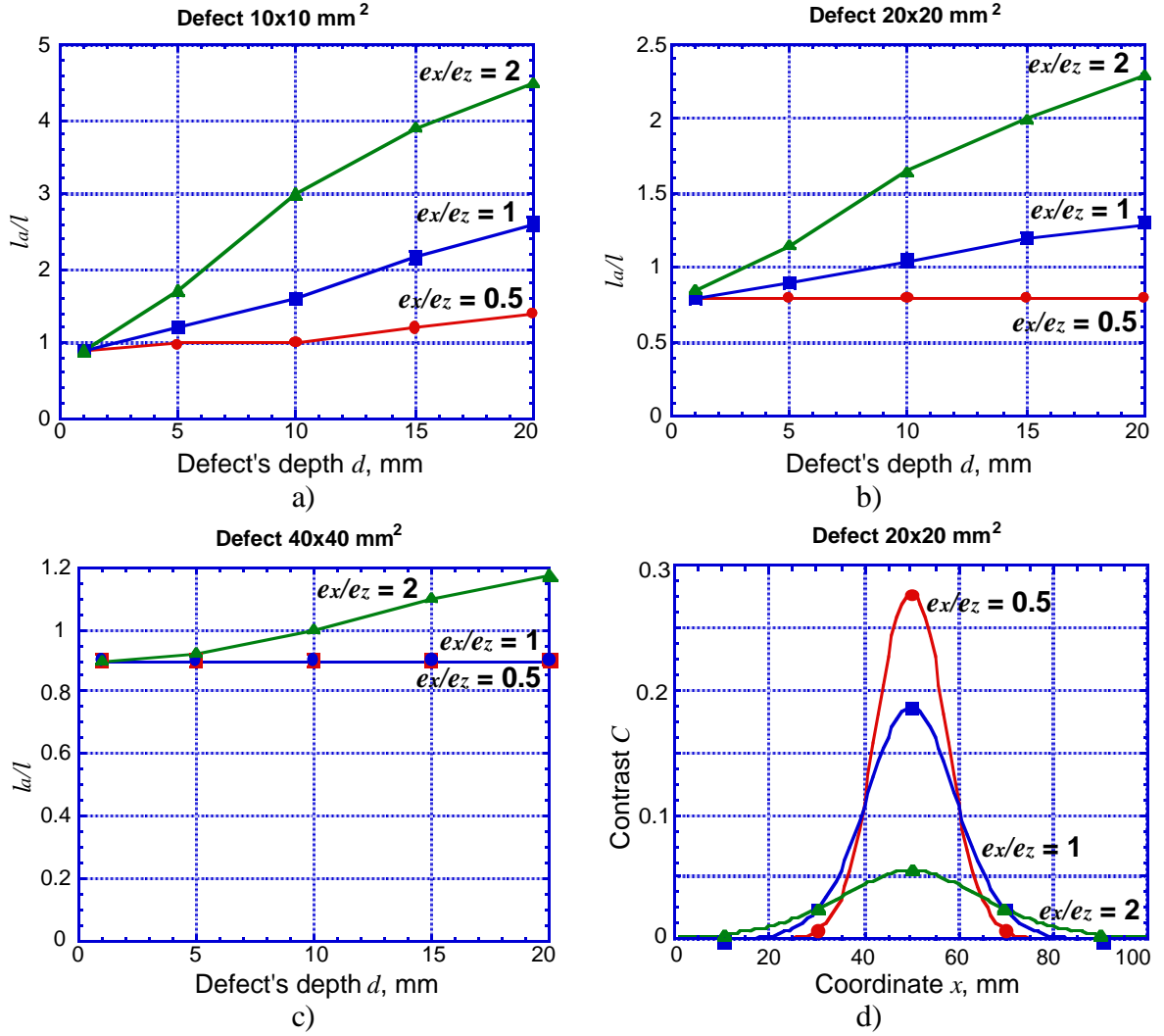
Figure 4. Influence of the thermal properties on the reconstructed size l_a/l when the original defect's size l is: a) 10 mm; b) 20 mm; c) 40 mm; d) thermal contrast above the defect 20 mm x 20 mm for different values of e_x/e_z.

Fig. 4d presents the contrast distribution on the surface above the 20 mm x 20 mm defect at 10 mm under the surface for different values of e_x/e_z (the actual defect extends from coordinate 40 to 60). Increasing the through the thickness diffusivity compared to the in-plane diffusivity increases the amplitude of the thermal contrast above the defect. Decreasing this ratio (which is typical for CFRP) results in a wider and smaller contrast profile. Therefore detection and reconstruction of a defect in an actual CFRP plate is more difficult than for isotropic materials.

EXPERIMENTS

The experiments with CFRP samples require a special development of hardware and software and are a subject for another paper. However, it is essential to verify the tomography algorithm with experimental data. In order to do this, the thermal response of a 25.4 mm thick plate of opaque plastic, has been used. The plate has square shape, 30 cm on a side. Nine square flat bottom holes with 25.4 mm on a side are milled into the back side of the plate on depth ranging from 12% to 94% of the total thickness of the plate. The experimental setup is described in detail in work [6]. The reconstruction algorithm has been applied to the infrared
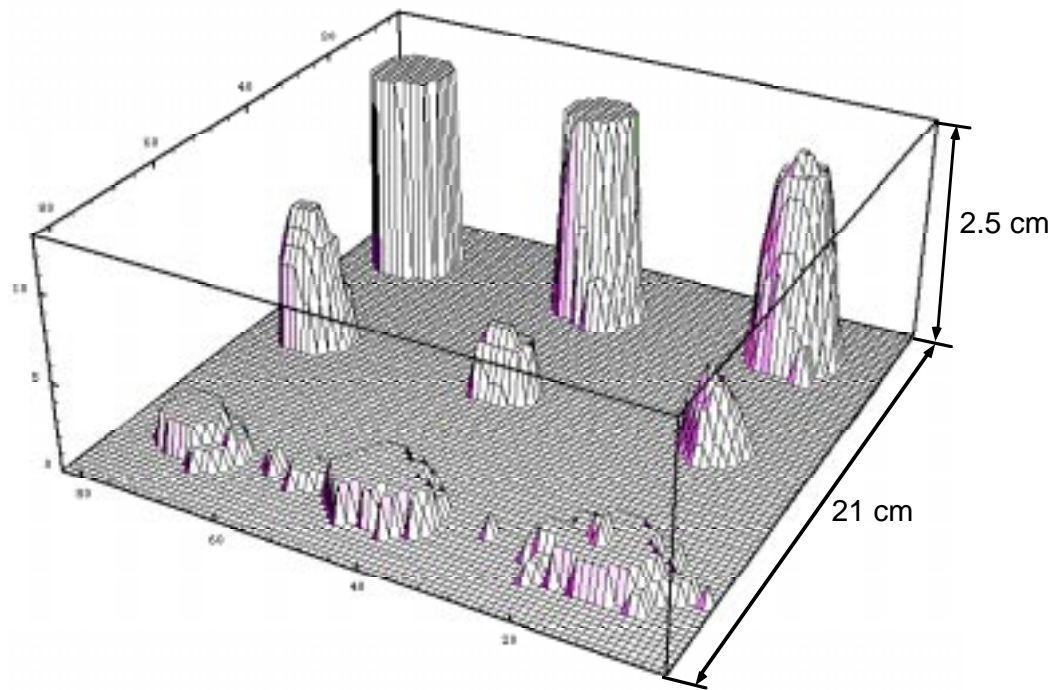
Figure 5. Reconstructed 3D image of the plate with 9 square flat bottom holes.

data from the plate. 13 tomograms for layers from the top surface down to the bottom have been reconstructed. Each tomogram contains binary information in array 85 x 85 pixels about 1.9 mm thick layer of the plate. The summarized three dimensions thermal tomography image of the plate is shown in Fig. 5 (the scales are different in horizontal and vertical directions). As could be seen from Fig. 5, the reconstruction method identifies all 9 holes and gives a reasonable approximation for depths. The reconstructed shape does not give an accurate representation of the shape of each hole in the specimen. However, the image in Fig. 5 is much easier to understand and less noisy than the original infrared image [6].

CONCLUSIONS

The influence of anisotropy on the reconstructed shape of defects has been investigated using a simulation of the thermographic process. Simulations of an "ideal" (noise free) thermal system confirms that the reconstruction algorithm is effective for CFRP structures. The reconstruction of defects in the structures gives an accurate indication of the location of the defect. However, except for the case of defects which are much larger that the depth of the defect, the size of the defect is over estimated by the reconstruction technique. The ratio of the size of the reconstructed defect to actual defect size increases as a given defect is located deeper in the material. The ratio also increases as the ratio of in-plane to through the thickness diffusivities increases. Within these limitations, the reconstruction process produces a concise presentation of the data that accurately indicates the existence and location of flaws in the structure.

ACKNOWLEDGMENTS

REFERENCES

1. V. Vavilov, X. Maldague, B. Dufort, F. Robitaille, and J. Picard, NDT & E International, Vol. 26, 2 (1993), pp. 85-95.
2. X. Maldague, *Nondestructive Evaluation of Materials by Infrared Thermography* (Springer-Verlag, London, 1993).
3. H.S. Carslaw and J.C. Jaeger, *Conduction of Heat in Solids*, 2nd ed. (Clarendon, Oxford, 1959).
4. W.J. Minkowicz, *Handbook of Numerical Heat Transfer* (Wiley, New York, 1988).
5. D.P. Almond, P. Delpech, M.H. Beheshtey, and P. Wen, in *Proceedings of the conference Nondestructive Evaluation of Materials and Composites:* SPIE Vol. 2944 (1996), pp. 256-264.
6. W.P. Winfree and K.E. Cramer, in *Thermosense XVIII: An International Conference on Thermal Sensing and Imaging Diagnostic Applications*, Proc. SPIE Vol. 2766 (1996), pp. 228-235.